www.nature.com/ismej

ISME

ARTICLE

Check for updates

Response to substrate limitation by a marine sulfate-reducing bacterium

Angeliki Marietou[1]✉, Kasper U. Kjeldsen[1], Clemens Glombitza[2] and Bo Barker Jørgensen[1]

Sulfate-reducing microorganisms (SRM) in subsurface sediments live under constant substrate and energy limitation, yet little is known about how they adapt to this mode of life. We combined controlled chemostat cultivation and transcriptomics to examine how the marine sulfate reducer, *Desulfobacterium autotrophicum*, copes with substrate (sulfate or lactate) limitation. The half-saturation uptake constant (K_m) for lactate was 1.2 µM, which is the first value reported for a marine SRM, while the K_m for sulfate was 3 µM. The measured residual lactate concentration in our experiments matched values observed in situ in marine sediments, supporting a key role of SRM in the control of lactate concentrations. Lactate limitation resulted in complete lactate oxidation via the Wood–Ljungdahl pathway and differential overexpression of genes involved in uptake and metabolism of amino acids as an alternative carbon source. *D. autotrophicum* switched to incomplete lactate oxidation, rerouting carbon metabolism in response to sulfate limitation. The estimated free energy was significantly lower during sulfate limitation (−28 to −33 kJ mol^{-1} sulfate), suggesting that the observed metabolic switch is under thermodynamic control. Furthermore, we detected the upregulation of putative sulfate transporters involved in either high or low affinity uptake in response to low or high sulfate concentration.

The ISME Journal (2022) 16:200–210; https://doi.org/10.1038/s41396-021-01061-2

INTRODUCTION

Sulfate reduction is a geologically ancient microbial metabolism, by which sulfate is converted to sulfide with concomitant oxidation of organic matter or H_2. Sulfate-reducing microorganisms (SRM) are abundant in marine coastal and shelf sediments, where sulfate is a main electron acceptor for the anaerobic mineralization of organic matter [1, 2]. The sulfate concentration decreases with sediment depth to a background of about 10 µM below the sulfate–methane transition zone (SMTZ) [3] where methanogenesis becomes the main, terminal carbon mineralization pathway [4]. However, despite the low sulfate concentration, SRM persist below the SMTZ and sulfate reduction proceeds in a cryptic sulfur cycle [5].

Electron donor limitation is the prevailing physiological state of most free-living heterotrophic microorganisms and this holds particularly true for the marine subsurface [6, 7]. Several possible mechanisms for adaptation to low-energy life in marine sediments have been suggested in the literature. Morphological changes, efficient ATP synthesis driven by a sodium rather than a proton motive force, decreased membrane permeability, and limited biomolecule decay are likely important characteristics for life in the deep subsurface that serve to minimize the maintenance requirements of cells [8, 9]. Known adaptations to low-energy conditions also include: (i) changes in the affinity of the enzymes involved in the uptake of the limiting substrate [10], (ii) switching the metabolism to incomplete oxidation of the energy source ("overflow" metabolism) under electron acceptor limitation [11], (iii) uncoupling of energy conservation pathways [11], and (iv) adopting a "multivorous" diet by scavenging and metabolizing a broader range of carbon sources simultaneously [12].

The majority of the information on the adaptation of microorganisms to energy limitation comes from pure culture experiments of aerobic or facultatively anaerobic microorganisms of biotechnological importance [11, 12]. There have been few efforts to characterize how natural populations adapt to the low-energy life in the marine subsurface in situ [13–16], and results from such studies are often difficult to interpret due to the ecological complexity of the study systems. Previous studies of SRM grown under controlled conditions of sulfate or electron donor limitation focused primarily on characterizing high-affinity uptake kinetics for the limiting substrate [17–25]. However, the physiological changes and molecular "rewiring" involved in the adaptation of SRM to substrate limitation remain a black box to be explored.

Our study aimed to understand how SRM in marine sediments adapt to substrate limitation, using the SRM *Desulfobacterium autotrophicum* HRM2 as a model organism. *D. autotrophicum* is a marine, complete oxidizer (which oxidizes the organic electron donor to CO_2) from the deltaproteobacterial family, Desulfobacteraceae [26]. The genome of *D. autotrophicum* has been sequenced and annotated [27], which, along with a proteomic analysis [28], offers a detailed genetic map of its metabolic potential. According to cultivation-independent analyses, Desulfobacteraceae dominate the SRM communities across the different geochemical zones in coastal marine sediments, including sulfate-rich surface sediments and the sulfate-depleted subsurface [29–31]. *D. autotrophicum* efficiently takes up sulfate at both mM and µM ambient concentrations, suggesting the presence of several sulfate uptake systems with different affinities

[1]Section for Microbiology, Department of Biology, Aarhus University, Aarhus, Denmark. [2]Institute of Biogeochemistry and Pollutant Dynamics, ETH Zürich, Zürich, Switzerland. ✉email: a.marietou@bio.au.dk

Received: 29 May 2020 Revised: 4 July 2021 Accepted: 6 July 2021
Published online: 20 July 2021

Table 1. Stoichiometry of lactate and sulfate utilization during steady state in chemostat cultures grown under either sulfate or lactate limitation.

Steady state	C_R Lac	C_R Sulf	C_R Acet	Sulf Used	Lac Used	S:L	csSRR	csLOR
LSR1	0.64 μM (0.08)	6.4 mM (0.1)	0.7 μM (0.2)	3.3 mM (0.1)	1.9 mM (0.1)	1.7	1.9 (0.1)	1.1 (0.1)
LSR2	<0.23 μM	6.2 mM (0.4)	<0.19 μM	2.6 mM (0.4)	2.1 mM (0)	1.3	1.6 (0.2)	1.3 (0)
SSR1	5 mM (0)	4.7 μM (0)	2.2 mM (0.9)	3.6 mM (0.1)	5.9 mM (0.1)	0.6	1.1 (0)	1.8 (0)
SSR2	4.1 mM (0.2)	2.6 μM (1.3)	3.0 mM (0.1)	3.5 mM (0)	6.3 mM (0.2)	0.5	1.59 (0.2)	2.9 (0.2)

LSR lactate steady-state replicate run, *SSR* sulfate steady-state replicate run, C_R *Lac* lactate residual concentration, C_R *Sulf* sulfate residual concentration, C_R *Acet* acetate residual concentration, *S:L* sulfate: lactate ratio, *csSRR* cell-specific sulfate-reduction rate (fmole per cell per day), *csLOR* cell-specific lactate oxidation rate (fmole per cell per day), *()* st dev of the mean of steady-state samples at different volume changes.

[32, 33], in agreement with the similar dual sulfate uptake kinetics observed in marine sediments [34]. We established a chemostat system for cultivating *D. autotrophicum* and used replicated steady-state cultures for chemical and transcriptomic analyses of its physiology when growing under substrate limitation. This allowed us to isolate the effects of electron donor (lactate) and electron acceptor (sulfate) limitation on its metabolism, including determining the apparent half-saturation uptake constants (K_m) for both substrates.

MATERIALS AND METHODS

Cultivation

D. autotrophicum HRM2 (DSM 3382^T) was grown anaerobically at 25 °C in a bicarbonate-buffered basal mineral medium [21] with sulfate as electron acceptor and lactate as electron donor and carbon source. Cells were grown either in batch (200 mL serum bottles) or continuous culture (chemostat) mode as described below. For sulfate-limitation experiments the culture medium contained 10.5 ± 0.2 mM lactate and 3.5 ± 0 mM sulfate, while for lactate-limitation experiments the medium contained 2.0 ± 0.1 mM lactate and 9.3 ± 0.4 mM sulfate (Table S1).

Chemostat operation

A 2 L glass bioreactor (Glasgerätebau Ochs; Bovenden, Germany) was used for continuous culturing. The reactor was sparged with a N_2/CO_2 gas mix (80:20) to maintain anaerobic conditions and operated under stirring at 200 rpm. The temperature (25 °C) was controlled by a water jacket and a cryostat bath (Lauda; Lauda-Königshofen, Germany) and monitored with a temperature probe (Mettler Toledo; Columbus, Ohio, USA). The pH of the reactor was monitored with a pH electrode (Mettler Toledo) and was maintained at 7.05 ± 0.05. The influent (medium) and the effluent (waste) were pumped with a turnover of 0.26 d^{-1} in the bioreactor with a peristaltic pump (Watson-Marlow; Falmouth, UK) with Viton (DuPont; Wilmington, Delaware, USA) pump tubing. Each experiment was performed twice and until steady-state was reached (Figs. S1, S2). Steady state was approached after four total volume changes where the optical density (OD_{600}), cell numbers (determined by using a BürkerTürk counting chamber), and residual substrate concentrations were stable. Any volume changes following steady state were considered a biological replicate (Figs. S1, S2). The lactate-limited chemostat was operated as a semi-open system, where part of the headspace was flushed out, while the sulfate-limited chemostat was operated as a closed system. The flushing removed sulfide and other gasses from the lactate-limited chemostat, the liquid phase nonetheless contained at least 0.4 mM sulfide and potential pH effects caused by the flushing were counteracted by the continuous pH adjustment.

Analytical procedures

Samples were periodically removed from batch and chemostat cultures in order to determine the concentration of different chemical species. Routinely lactate, acetate, succinate, formate, pyruvate, propionate, butyrate, acetoin, glucose, fumarate, glycerol, and ethanol were measured by high-pressure liquid chromatography (>100 μM) [35], while low lactate/acetate concentrations (<100 μM) were measured by two dimensional ion chromatography-mass spectrometry [36] (Table S2). Sulfate was measured by suppressed ion chromatography (limit of detection 0.5 μM) in samples sparged with CO_2 to strip off hydrogen sulfide [37]. Sulfide concentrations were determined spectrophotometrically at 670 nm in zinc-preserved samples by the methylene blue method with a detection limit of 0.5 μM [38].

Transcriptomic analysis

Samples (200 mL) from duplicate chemostat cultures at steady state were collected directly into sterile vials containing an equal volume of the RNA-stabilizing reagent RNA Later (Merck; Kenilworth, New Jersey, USA). Preserved cells were harvested by centrifugation at 10,000 rpm for 20 min and pellets were immediately stored at −80 °C. The cell pellets were resuspended in 3.5 ml phenol-chloroform-isoamyl alcohol and RNA was extracted with the MoBio RNA PowerSoil Total RNA Isolation kit (Qiagen; Hilden, Germany). All samples were subsequently treated with Turbo DNase (Ambion; Austin, Texas, USA) to remove any residual DNA contamination. The absence of DNA contamination was confirmed by qPCR quantification of 16S rRNA gene copy numbers [39]. Removal of rRNA (Ribo-zero magnetic kit; Illumina; San Diego, California, USA), library preparation (TrueSeq Stranded Total RNA kit; Illumina), and sequencing (HiSeq2500, SR50 reads, Illumina) were performed with a commercial service (DNASense, Aalborg, Denmark). The resultant reads (>22 million per sample) were mapped onto the genome of *D. autotrophicum* HRM2 (accession number NC_012108) with BBmap version 34.94 with default mapping parameters. The subsequent data analysis (described in detail in SI Materials and Methods) was performed as described previously [40]. The most highly expressed genes were identified and ranked by converting mapping data into reads per kilobase pair per million (RPKM). The average coverage was 22× and 166× for the sulfate replicates and 23× and 181× for the lactate replicates per run. Pearson correlation coefficients (*r*) of gene expression levels of replicate samples were between 0.87 and 0.81 indicating good reproducibility (Fig. S3). The transcriptome sequence data have been deposited in the Sequence Read Archive under accession numbers SRX8129177–SRX8129180.

Comparative genomics

The closed genomes of 41 sulfate-reducing bacteria and 5 sulfate-reducing archaea (Table S3) were manually examined for the presence of two-component regulatory systems associated with putative sulfate transporters as identified by the transcriptomic analyses of *D. autotrophicum*. Homologs of the putative sulfate transporters or other proteins of interest were identified by blastp search. All analyses were performed with the IMG/MER online database (accessed November 2020) [41].

RESULTS AND DISCUSSION

Steady-state growth under lactate or sulfate limitation

D. autotrophicum was grown in the chemostat with a doubling time of 4 days and a dilution rate of 0.26 d^{-1} at 25 °C under lactate-limitation (excess sulfate) or sulfate limitation (excess lactate). This dilution rate constitutes 34% of the maximal growth rate of *D. autotrophicum* (0.755 d^{-1}) when grown in batch culture under similar conditions. Steady state was reached after 16 days of growth in the chemostats (four volume changes), after which point residual substrate concentrations remained constant (Figs. S1, S2). Under lactate limitation, lactate was completely oxidized to CO_2 as confirmed by (i) the 2:3 stoichiometry (Eq. 1) between lactate and sulfate consumption and (ii) the sub-μM steady-state concentrations of both residual lactate and acetate (Table 1).

$$2CH_3CHOHCOO^- + 3SO_4^{2-} \rightarrow 6HCO_3^- + 3HS^- + H^+ \quad (1)$$

Complete lactate oxidation yields 12 electrons, while the reduction of sulfate to sulfide requires 8 electrons. In agreement, at steady state the cells reduced on average 1.5 mol of sulfate for

Table 2. Substrate affinity constants for lactate-utilizing sulfate-reducers.

Organism	μ (d^{-1})	K_{mLac} (μM)	K_{mSulf} (μM)	B/C[a]	F/M[b]	Reference
Desulfovibrio desulfuricans	8.6	49	ND	C	F	[17]
Desulfovibrio desulfuricans ATCC 5575	9.2	16	ND	C	F	[22]
Desulfovibrio desulfuricans ATCC 5575	8.3	ND	19	C	F	[23]
Desulfovibrio desulfuricans	1.6[c]	ND	5	B	F	[85]
Desulfovibrio vulgaris (Marburg)	5.5	ND	10	C	F	[19]
Desulfovibrio vulgaris (Hildenborough)	0.83[c]	ND	32	B	F	[86]
Desulfovibrio sapovorans	0.8[c]	ND	7.3	B	F	[86]
Desulfovibrio salexigens	2.8[c]	ND	77	B	M	[86]
Desulfobacter postgatei	ND	ND	200	B	M	[20]
Thermodesulfobacterium sp. strain JSP	3.1[c]	ND	3	B	F	[44]
Thermodesulfovibrio sp. strain R1Ha3	0.9[c]	ND	3	B	F	[44]
Desulfobacterium autotrophicum	0.8[c]	ND	8	B	M	[32]
Desulfobacterium autotrophicum	0.3	1.2	3	C	M	This study

[a]B/C: batch (B) or continuous (C) culture.
[b]F/M: freshwater (F) or marine (M).
[c]Maximum specific growth rate in batch cultures.

every mol of lactate oxidized (Table 1). The K_m for lactate uptake was calculated using the modified Monod model: $\mu = \mu_{max} \cdot S/(K_m + S)$, where μ_{max} is the above-mentioned maximum specific growth rate determined in batch culture, μ is the specific growth rate in the chemostat which equals the dilution rate of the chemostat, and S is the residual steady-state substrate concentration in the chemostat. The K_m for lactate (1.2 μM) in *D. autotrophicum* was considerably lower than the few previously reported lactate K_m values for SRM isolates (16 and 49 μM; Table 2) and is the first reported such K_m value for a marine SRM isolate. The residual steady-state concentration of lactate ranged from 0.6 μM to below the detection limit of 0.23 μM (Table 1). These concentrations are well below the lactate concentrations measured in marine sediments from Aarhus Bay (Denmark), Godthåbsfjord (Greenland), and the Baltic Sea (Table 3, Fig. S4). In all these sediments, lactate is present within a narrow concentration range of 0.9–3.0 μM with a mean of 1.6 μM (±0.6). Lactate is the most widely used substrate by known cultivated SRM [42] and sediment slurry experiments have demonstrated that when sulfate reduction is inhibited there is an almost complete inhibition of lactate turnover [43]. Our observed K_m value for lactate suggests that SRM could potentially control the in situ lactate concentration.

Under sulfate limitation, the steady-state concentration of sulfate was 4.7 and 2.6 μM during the two runs (Table 1). A similarly low residual sulfate concentration of 2 μM was also described previously in batch experiments with thermophilic freshwater SRM isolates [44]. The K_m for sulfate in *D. autotrophicum* (3 μM) is similar to the reported K_m values for marine sediments and for previous batch culture experiments with *D. autotrophicum* [32, 34]. The concentration of sulfate in marine sediments decreases with depth from a seawater value of 28 mM at the sediment–water interface to a background of around 10 μM below the SMTZ [3]. SRM maintain active sulfate reduction over this entire concentration range [3, 29, 31]. Even though the calculated csSRR (cell-specific Sulfate Reduction Rate) of the *D. autotrophicum* chemostat culture is tenfold higher (Table 1) than the csSRR inferred for marine surface sediments (0.1 fmol $cell^{-1}$ day^{-1}) [ref. 7, 29], the residual substrate concentrations for lactate and sulfate fall within the range of in situ substrate concentrations, rendering our continuous culture representative of substrate limitation in marine sediments.

Table 3. In situ lactate concentrations in marine sediments.

Sampling site	Lactate (μM)[a]	Reference
M1 station, Aarhus Bay	2.08 (0.6)	[36]
M5 station, Aarhus Bay	1.30 (0.7)	This study
S3, Godthåbsfjord, Greenland	0.93 (0.4)	This study
S6, Godthåbsfjord, Greenland	1.16 (0.8)	This study
S8, Godthåbsfjord, Greenland	0.90 (1.0)	This study
M59C, Baltic Sea	2.96 (2.6)	This study
M63E, Baltic Sea	1.65 (1.6)	This study
M56C, Baltic Sea	1.72 (1.5)	This study

The depth concentration profiles can be found in Fig. S4.
() Standard deviation of the mean.
[a]Average value across different depths.

Stoichiometry under sulfate limitation

Even though *D. autotrophicum* is a complete oxidizer under lactate limitation, we observed the accumulation of 2–3 mM acetate under sulfate limitation (Table 1). According to the expected stoichiometry shown in Eq. (2) [45] during the incomplete oxidation of 1 mol lactate in SRM of the *Desulfovibrio* genus, 0.5 mol sulfate is reduced and 1 mol acetate is produced.

$$2CH_3CHOHCOO^- + SO_4^{2-} \rightarrow 2CH_3COO^- + 2HCO_3^- + HS^- + H^+ \quad (2)$$

However, we observed the accumulation of 3 ± 0.1 mM acetate, instead of the expected 6.2 ± 0.2 mM for the incomplete oxidization of 6.2 ± 0.2 mM of lactate and reduction of 3.6 ± 0.1 mM sulfate (Tables 1, S1). No nongaseous products were detected (≥0.1 mM) other than acetate.

One possible explanation for this discrepancy could be the presence of a heterogeneous population in the chemostat, where a fraction of the cells grew via sulfate reduction and complete lactate oxidation (Eq. 1), while another fraction grew via lactate fermentation. According to this scenario, and based on the substrate stoichiometries observed, we would expect that the 3.6/3.5 mM (SSR1/SSR2) sulfate, which was reduced, would consume 2.4/2.3 mM (SSR1/SSR2) of lactate by its complete oxidation, while the remaining of the used lactate, 3.5/4 mM (SSR1/SSR2), would be converted completely to acetate (Table 1; Eq. 3).

$$CH_3CHOHCOO^- + H_2O \rightarrow CH_3COO^- + CO_2 + 2H_2 \quad (3)$$

The measured 2.2/3 mM (SSR1/SSR2) acetate still differed from the expected 3.5/4 mM (SSR1/SSR2) values according to this

scenario. Even though *D. autotrophicum* can ferment lactate in the absence of a terminal electron acceptor, we propose that the observed discrepancy in the expected stoichiometry is due to electron acceptor/nutrient limitation. This is a previously characterized response known as "overflow" metabolism [11].

"Overflow" metabolism has been observed in unicellular organisms, when grown in the presence of high electron donor concentrations, and is due to inefficient metabolic pathways and the spilling of energy resources [46]. *Saccharomyces cerevisiae*, *Escherichia coli*, *Bacillus subtilis*, and *Klebsiella aerogenes* incompletely oxidize glucose via energy-spilling catabolic pathways at high glucose concentrations and fully oxidize glucose at low glucose concentrations [46]. *E. coli* accumulates acetate in the presence of oxygen when the rate of glucose consumption is too high due to the enzymatic limitation of the tricarboxylic acid cycle. As a result, the carbon flux from acetyl-coenzyme A is directed to acetate instead of entering the tricarboxylic acid cycle, thereby accumulating metabolic intermediates to maintain the cell's redox balance [47].

We therefore propose that, under sulfate limitation, the rate of lactate consumption in *D. autotrophicum* is greater than its capacity to reoxidise the reduced equivalents generated, resulting in "overflow" metabolism and rerouting of carbon metabolism. Approximately 50% of the lactate is incompletely oxidized to acetate, while the other 50% is directed through the Wood–Ljungdahl Pathway (WLP) and oxidized to CO_2 with the excess reducing equivalents converted to H_2 (electron sink) as described in Eq. (4).

$$2CH_3CHOHCOO^- + SO_4^{2-} + 4H_2O \rightarrow CH_3COO^- + 4HCO_3^- + HS^- + 2H^+ + 4H_2 \quad (4)$$

The marine thermophilic SRM, *Archaeglobus fulgidus*, similarly switch from complete to incomplete lactate oxidation upon sulfate limitation in chemostat experiments [24]. A metabolic switch was also observed in *Desulfovibrio alaskensis*; under sulfate excess, pyruvate was completely oxidized to acetate, while under sulfate limitation pyruvate was oxidized to acetate and reducing equivalents in the form of H_2 [48]. In our experiments this scenario is further supported by the observed lactate:sulfate ratio (0.6) and the absence of additional non-gaseus products other than acetate (Tables 1, S1). Moreover, the cell-specific lactate oxidation rate was higher under sulfate limitation than under lactate limitation, as well as higher than the csSSR under sulfate limitation (Tables 1, S1), further supporting the "overflow" hypothesis.

Noguera et al. proposed the presence of two electron transport pathways that operate simultaneously in *Desulfovibrio* sp. According to their presented model, one mechanism transports the electrons generated from lactate oxidation directly through membrane-bound electron carriers to sulfate, while the second mechanism involves H_2 [49]. Odom and Peck [50] originally suggested the involvement of H_2 in the transport of electrons from the organic donor to sulfate in SRM. Lupton et al. [51] further argued that H_2 is produced as a spilling reaction in SRM when the production of electrons from an organic donor exceeds the rate at which these electrons can be taken up by the sulfate-reduction pathway. The model presented by Noguera et al. estimated that 48% of the electrons transported from lactate to sulfate involved H_2 production, which further supports our observed stoichiometries under sulfate limitation.

Energetics of substrate limitation

Under lactate limitation, the free energy available at steady state for sulfate reduction was estimated to be −81 to −76 kJ mol^{-1} sulfate (Table S1). The estimated free energy was lower during sulfate limitation (Eq. 4), estimated to be −28 to −33 kJ mol^{-1} sulfate (Table S1) under otherwise similar conditions. The estimated free energy under sulfate limitation is consistent with laboratory-based (33–43 kJ mol^{-1} sulfate) [52] and in situ observations (31 kJ mol^{-1} sulfate) [37]. This may identify the minimum energy requirement for sulfate reduction and suggests that the observed substrate stoichiometry of the sulfate-limited chemostats are under thermodynamic control. The existence of dual electron transport pathways, allowing for hierarchical routing of the carbon metabolism, could be key to the adaptation and survival over a wide range of sulfate concentrations observed for SRM. We propose that the metabolic "switch" from complete lactate oxidation under excess sulfate to incomplete lactate oxidation and "overflow" metabolism under sulfate limitation is under thermodynamic regulation in response to the in situ sulfate concentration, as predicted by Noguera et al.

Transcriptional response to substrate limitation

We employed a transcriptomic approach to identify the metabolic pathways involved in the response of *D. autotrophicum* to lactate or sulfate limitation. The majority of the *D. autotrophicum* genes did not alter their pattern of expression during steady-state growth under the two tested conditions (Fig. 1A). The use of chemostat-grown cells minimized gene expression effects that could be due to differences in growth rate, growth phase, or transition stage between the two tested conditions [53]. Following normalization of transcript abundances by conversion to RPKM values to account for differences in sequence library size and gene length, and a strict statistical analysis ($p < 0.001$), we identified 24 and 79 genes that were ≥2-fold overexpressed under lactate and sulfate-limitation, respectively (Fig. 1B). The differentially overexpressed genes clustered on the same or on neighboring operons (Table S4), as expected for genes under the control of the same transcriptional regulators or involved in the same functions [54].

The top 20 most highly expressed genes were the same under both lactate and sulfate limitation, with the exception of the *lld*P, a L-lactate permease encoding gene, that was only highly expressed under lactate-limitation (Table S5). Several of the highly expressed genes are involved in the sulfate-reduction pathway. The dissimilatory reduction of sulfate to sulfide is a multistep process with an initial ATP-dependent activation of sulfate to adenosine-5′-phosphosulfate (APS) by ATP sulfurylase (*sat*), followed by the reduction of APS to sulfite by APS reductase (*apr*AB), and finally the reduction of sulfite to sulfide by dissimilatory sulfite reductase (*dsr*AB) and the protein DsrC (*dsrC*), all of which were highly expressed (Table S5). The genes of this pathway are among the most highly and constitutivly expressed genes in SRM [42, 45, 55]. Besides the genes for sulfate reduction, several genes involved in electron-transfer processes were highly expressed, including rubrerythrin, flavodoxin, and FeS-proteins and a cytochrome (Table S5). The latter cytochrome (HRM2_42360) is a putative class III cytochrome c that in cytochrome-rich SRM like *D. autotrophicum*, along with other multiheme cytochromes, acts as electron shuttles between soluble periplasmic hydrogenases and several membrane complexes [28]. In other Desulfobacteraceae constitutive expression of similar proteins (50% identity) suggested a key role in general energy metabolism [28], possibly acting as shuttle for electrons between the different alternative energy generating pathways allowing for higher metabolic flexibility [42, 56].

A gene (HRM2_17810) encoding an ATP synthase F0 subcomplex C subunit, which forms the rotor of the ATP synthase, was highly expressed under both lactate and sulfate-limited growth (Table S5) as a high number of c subunits is required for a functional F0 rotor [57]. Upregulation of genes encoding for the F0 beta subunit was observed under sulfidogenic metabolism when compared to syntrophic metabolism in *D. vulgaris* [58]. We did not observe any significant change on the expression of the ATP synthase F0 subunits between lactate limitation and sulfate limitation which suggests that *D.*

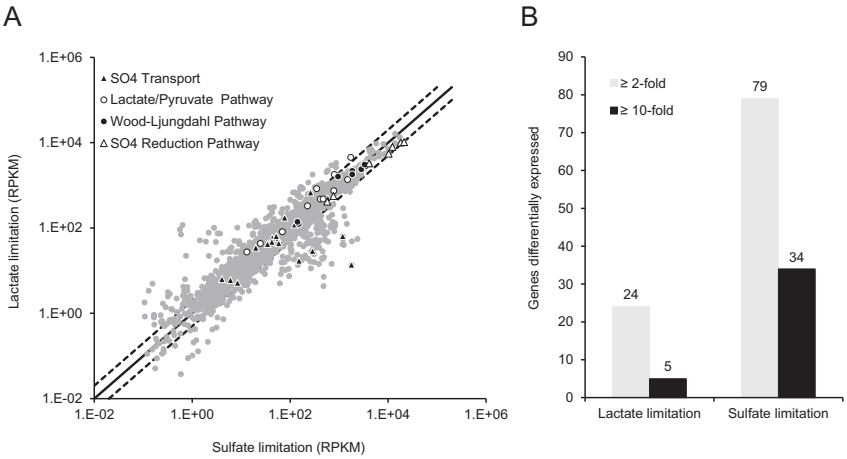

Fig. 1 Gene expression of *D. autotrophicum* during growth by lactate- and sulfate limitation. A Genes are represented by dots and are positioned according to their RPKM (reads per kilobase pair per million) expression values. Genes relevant to this study are pattern-coded (see legend). **B** Number of genes significantly differentially overexpressed at the tested conditions ($p < 0.001$).

autotrophicum did not switch to lactate fermentation under sulfate-limitation.

Interestingly, two genes encoding for cold-shock DNA-binding proteins were also among the highest expressed genes (Table S5). Cold-shock proteins CspL and CspB function as RNA chaperones and are key for adaptation to cold and to survival at stationary phase in *Bacillus subtilis* [59]. Since the optimum growth temperature for *D. autotrophicum* is 25–28 °C [26, 60], we speculate that the high numbers of transcripts for cold-shock proteins are related to a low substrate availability response commonly encountered at stationary phase [59].

Lactate-limitation specific response. In *D. autotrophicum*, lactate is oxidized to pyruvate by lactate dehydrogenase (*ldh*AB), while pyruvate is oxidatively decarboxylated by pyruvate:ferredoxin oxidoreductase (Por) to acetyl-CoA, which is then completely oxidized to CO_2 via the WLP [27, 28]. During steady-state growth under lactate limitation the genes encoding for lactate transporters, lactate dehydrogenases, and pyruvate:ferredoxin oxidoreductases (Fig. 1A) were not differentially expressed, in agreement with a previous proteomic study suggesting their constitutive expression irrespective of the electron donor source [28, 45]. However, HRM2_28740 encoding a proton-driven monocarboxylate transporter was fourfold upregulated (Table S4). Even though, HRM2_28740 is annotated as a oxalate/formate antiporter, it shares 29% identity with a lactate transporter (Sfum_3364) from *Syntrophobacter fumaroxidans*, suggesting a possible role for HRM2_28740 in lactate transport under lactate limitation (Fig. 2).

The previously identified genes of the WLP were not differentially expressed under lactate limitation (Fig. 1A). We identified a fivefold increase for two putative methylene-tetrahydrofolate reductase (*met*F) genes (HRM2_30860, MetF3; HRM2_30900, MetF4) and a threefold increase for a putative acetyl-CoA synthetase (AcsA1, HRM2_28720) (Fig. 2). The transcript abundance for metF3/4 (RPKM 922/839) was significantly higher compared to the *met*F1 (RPKM 124) and the transcript abundance for *acs*A1 (RPKM 3329) was higher compared to the *cdh*DE (RPKM 2386/2780) under lactate limitation (Tables S6, S7). This suggests that these isoenzymes may prevent WLP reversal, channeling all the acetyl-CoA through the WLP and thereby avoiding acetate build-up in the cell and loss via excretion.

The differential overexpression during lactate limitation of genes encoding for high-affinity branched-chain amino acid transporters and genes encoding for enzymes of (i) the leucine degradation (or biosynthesis) pathway (2-isopropylmalate synthase, LeuA2/A3; acetolactate synthase, IlvH/G; dihydroxy-acid dehydratase, IlvD) and (ii) the deamination of cysteine to pyruvate (D-cysteine desulhydrase, DcyD2) suggest that branched amino acids can act as alternative energy/carbon sources for *D. autotrophicum* in the environment (Fig. 2, Table S4). Two out of the three branched amino acids (leucine and isoleucine) are ketogenic; they can be degraded directly to acetyl-CoA, which can be "fed" to the WLP [61]. Upregulation of genes encoding such amino acid transporters may be a general response to electron donor limitation. We reanalysed the transcriptomic data for *Desulfovibrio alaskensis* [48] growing in chemostats under pyruvate limitation in the presence of excess of sulfate and found an amino acid transporter was among the most highly (8-fold) overexpressed genes (Table S8). Overexpression of high-affinity branched-chain amino acid transporter-encoding genes was also observed in glucose-limited cultures of *E. coli* [62, 63]. The genome of *D. autotrophicum* encodes for several extracellular or membrane-associated proteases that were expressed under the tested conditions (Table S9), suggesting that protein degradation is important for adaptation to energy-limitation in *D. autotrophicum*.

Sulfate limitation-specific response. Under sulfate limitation we observed the overexpression of four genes encoding for universal stress proteins (Table S4). Universal stress proteins are expressed in response to various unfavorable conditions including sulfate starvation [64]. Three (HRM2_40210-40220, HRM2_46590) out of the four overexpressed genes are similar (30% amino acid identity) to UspA-encoding genes from *D. vulgaris*, predicted to modulate the cell's response to growth phase transition and nutrient limitation [65]. Thus, the overexpressed *uspA* genes in *D. autotrophicum* could mediate the response to sulfate-limitation.

We also observed an eightfold overexpression of a gene encoding a putative acetyl-CoA synthetase (Acs, HRM2_46160) (Fig. 2, Table S4). Eleven paralogs of acetyl-CoA synthetase (acs) genes have been identified in the genome of *D. autotrophicum* [27], allowing *D. autotrophicum* to respond to changing environmental conditions by using different isoenzymes [27, 28, 66]. The Acs paralogue HRM2_46160 was not detected in the proteome of *D. autotrophicum* when batch cultures were grown on 8 different electron donors with excess sulfate, including autotrophic growth [28], thereby suggesting a unique role for this paralogue during sulfate limitation.

Under low sulfate concentrations, *D. autotrophicum* switches to incomplete oxidation, lactate is oxidized to pyruvate, which in turn is oxidatively decarboxylated to acetyl-CoA, thereby increasing the intracellular acetyl-CoA level [67]. A putative pyruvate dehydrogenase complex (HRM2_47610, HRM2_47620, and HRM2_47640) was

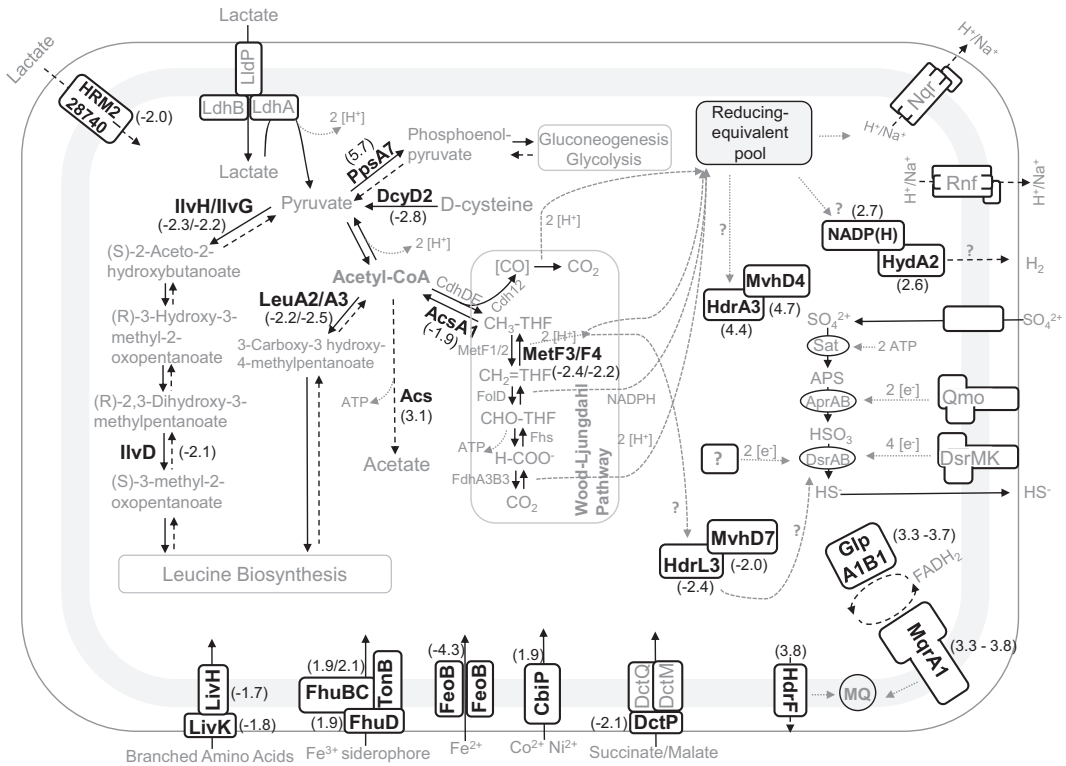

Fig. 2 Metabolic network of *D. autotrophicum* reconstructed from the differential overexpressed gene analysis. Proteins encoded by the overexpressed genes are highlighted in black. Putative pathways are indicated by dashed lines (black for metabolic pathways and gray for reducing equivalents). Protein names and their predicted functions are provided in Table S4. Negative parenthesis values represent log(2) fold change under lactate limitation, while positive values represent log(2) fold change under sulfate limitation.

5- to 8-fold overexpressed under sulfate limitation, possibly in response to the excess lactate and the high lactate turnover rates observed (Tables 1, S4). The transcript abundance of HRM2_47610, HRM2_47620, and HRM2_47640 were significantly higher compared to the constitutive pyruvate:ferredoxin oxidoreductases [28] PorA4 and PorB2 (Tables S6, S5). Moreover, pyruvate dehydrogenases are dependent on NAD^+ while pyruvate:ferredoxin oxidoreductases are ferredoxin dependent, suggesting that the switch is related to redox balancing [68]. As the uptake of lactate exceeds the cell's capacity to catabolize it, the system is balanced by the conversion of acetyl-CoA to acetate and its excretion to the environment (Fig. 2), in agreement with our observed stoichiometries under sulfate limitation (Table 1). Similar flux-sensing responses have been described in *E.coli* during "overflow" metabolism, allowing the cell to recognize metabolic "bottlenecks" by integrating information on the available substrates and transcriptionally or post-translationaly regulate several functionally different isoenzymes, depending on the growth condition such as the amount of electron donor or acceptor available [69].

A soluble cytoplasmic hydrogenase (HRM_26580, HydA2) was overexpressed (6-fold) under sulfate-limitation (Fig. 2, Table S4). The [FeFe] family hydrogenase is located upstream and co-transcribed with a NADPH-dependent oxidoreductase (HRM2_26590) that could interact with HydA along with ferredoxin for the production of H_2 (Fig. 2, Table S4). A similar electron-bifurcating [FeFe] hydrogenase has been described in *Thermotoga maritima*, which catalyzes the formation of H_2 with reduced ferredoxin only in the presence of NADH [70]. Constitutive hydrogenases in SRM could produce H_2 whenever an imbalance occurred between reductants produced and consumed in the cell [71]. Genes encoding for a periplasmic hydrogenase (HysAB; HRM2_11680-690) were highly expressed under both conditions and has been previously detected in the proteome of *D. autotrophicum* during chemolithotrophic growth [28]. Overexpression under sulfate limitation of the bifurcating [FeFe] hydrogenase HydA offers further evidence that SRM operate dual pathways in response to sulfate availability, driving the release of electrons as H_2 when sulfate availability is limited [48, 49, 71].

Electron-transfer components. The electron-transfer pathways of sulfate respiration are incompletely understood despite significant advances [56, 72], not least for *D. autotrophicum* [27, 28]. *D. autotrophicum*'s genome encodes for two Rnf complexes (membrane-localized ferredoxin:NAD^+-oxidoreductase) and a Nqr complex (Na^+-potential forming NADH:quinoneoxidoreductase), both of which were expressed under the tested conditions (Fig. 2) and believed to be involved in energy conservation (H^+/Na^+-based bioenergetics) in SRM [28, 56]. Soluble electron transfer components such as heterodisulfide reductases (HDR) can be found in nearly all SRB genomes. The highest numbers of HRD are found in the genomes of metabolically versatile SRM such as *D. autotrophicum* and encode for 15 heterodisulfide reductase (HDR) paralogues [27]. HDR are key enzymes in methanogens and other anaerobes, catalyzing electron-bifurcation reactions by a complex consisting of a HDR and a F420-nonreducing hydrogenase (Mvh) [73]. In SRM they are predicted to be involved in energy conservation though flavin-based electron bifurcation, but their exact role remains unclear [74]. Under lactate-limitation, a gene encoding for a soluble heterodisulfide reductase paralogue (*hdr*L3, HRM2_30890) was fivefold overexpressed (Table S4). The HdrL3-encoding gene is located downstream of the MvhD7- encoding gene (HRM2_30880), most likely forming a HdrL3/MvhD7 complex (Table S4, Fig. 2). HdrL is a fusion heterodisulfide reductase originally described in *D. autotrophicum*, with a previously uncharacterized role in electron cycling [28]. The genes encoding the HdrL3/MvhD7 complex are found on the same transcriptional

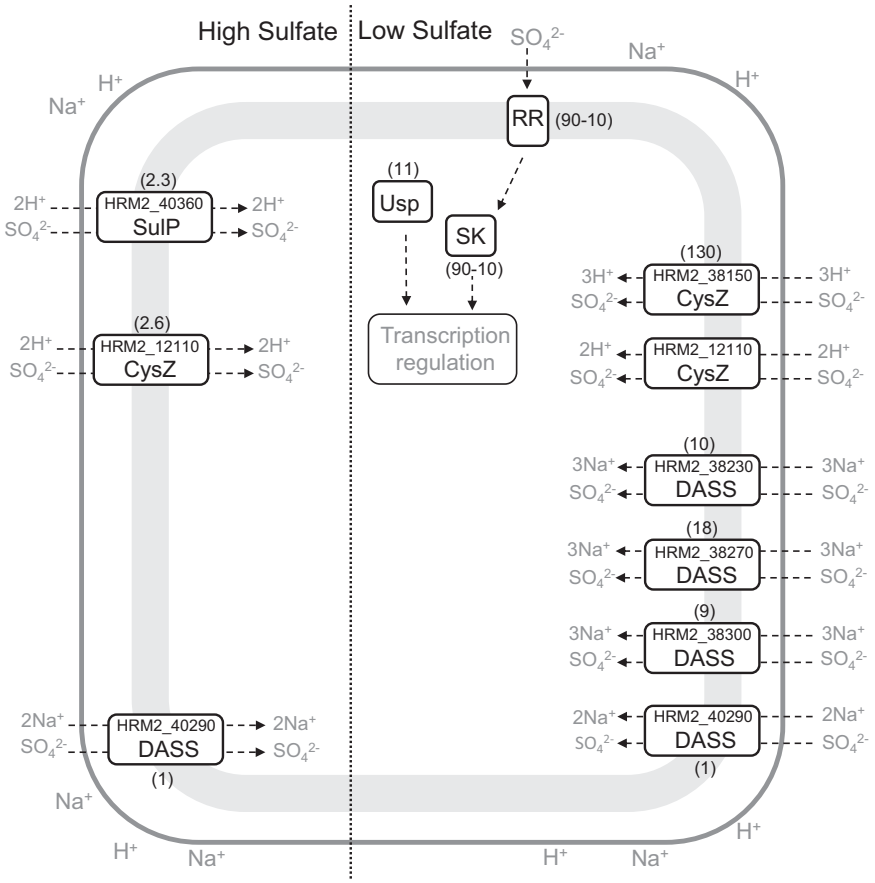

Fig. 3 Sulfate transport in *D. autotrophicum* under sulfate excess and sulfate-limited conditions reconstructed from the differential overexpressed gene analysis. Protein names and their predicted functions are provided in Table S4. SK Sensory kinase, RR response regulator. Values in parenthesis represent the fold change in expression.

unit as two methylene-tetrahydrofolate reductase genes (*met*F3/4) from the WLP, suggesting a possible role for the HdrL3/MvhD7 complex in the transfer of electrons from the WLP to the sulfate-reduction pathway under lactate limitation (Fig. 2, Table S4).

During sulfate limitation we observed a 13-fold overexpression of a gene (HRM2_03190) encoding the membrane-bound multi-domain HdrF1 protein previously proposed to be involved in electron transfer with the menaquinone pool and energy conservation [28, 74] (Table S4). Similarly, we observed a 5-fold overexpression of the HdrA3- and MvhD4-encoding and co-transcribed genes (Fig. 2, Table S4) [75]. We speculate that the HdrA3/MvhD4 complex plays an important role in cytoplasmic electron transfer during sulfate limitation as it was not detected in earlier differential proteomic analyses of *D. autotrophicum* under eight different substrates present in excess [28]. Another set of genes, overexpressed (13-fold) under sulfate-limitation and in close proximity to the *hdrF1* encoding gene, is a paralog of glycerol-3-phosphate dehydrogenase (GlpAB) (Fig. 2, Table S4). GlpAB is involved in cytoplasmic FADH reoxidation, while the generated electrons are transferred to the membrane menaquinone pool via the similarly overexpressed membrane quinone reductases, MqrA1 (HRM2_03200) and MqrA2 (HRM2_07780) [28] (Fig. 2, Table S4). Overexpression of the GlpAB and MqrA1/A2 encoding genes could be linked to the "overflow metabolism" in the presence of excess electron donor The remaining major electron-transfer protein complexes encoded in the *D. autotrophicum* genome [27, 28] were expressed to similar levels when comparing the two tested conditions (Table S7). The presence of HDR complexes that are differentially expressed between sulfate excess and sulfate limitation supports the idea that different electron-transfer pathways operate in SRM in response to changes in the environment.

The molecular basis of dual sulfate uptake kinetics. The most highly differentially-expressed (136-fold) gene under sulfate limitation encodes for *cys*Z (HRM2_38150), a TSUP (Toluene Sulfonate Uptake Permease) family putative sulfate transporter (Fig. 3, Table S4). Downstream, three more genes (*nadC1-3*) with a putative sulfate transport function were also highly (9 to 19-fold) overexpressed under sulfate limitation (Fig. 3, Table S4). Similarly, among the most highly overexpressed genes of *D. alaskensis* [48] under sulfate limitation was a NadC encoding gene (12-fold) offering further evidence for the key role of this family of transporters in low sulfate environments (Table S8). The ability of *D. autotrophicum* to switch to a high-affinity sulfate uptake system under sulfate-limitation has been previously described [32, 76]. The genome of *D. autotrophicum* encodes three paralogues of the SulP family, five paralogues of the NadC/DASS family, a member of the CysP family, and ten paralogues of the CysZ/TSUP family of sulfate transporters (Fig. 4A) [33]. Among the five paralogues of NadC, two were constitutively expressed, as previsoulsy shown by qPCR [32]. Moreover, two out of the three SulP paralogues were constitutively expressed and one appeared to be induced (twofold) by excess sulfate (Figs. 3, 4A). Putative SulP and NadC sulfate transporters have been consistently recovered in proteomic and transcriptomic studies of SRM grown under sulfate excess [28, 45, 63, 77], confirming a key role for SulP and NadC transporters in high sulfate environments.

A TSUP family putative sulfate transporter was also upregulated (2.5-fold) in *D. alaskensis* grown under sulfate excess (Table S7). Our

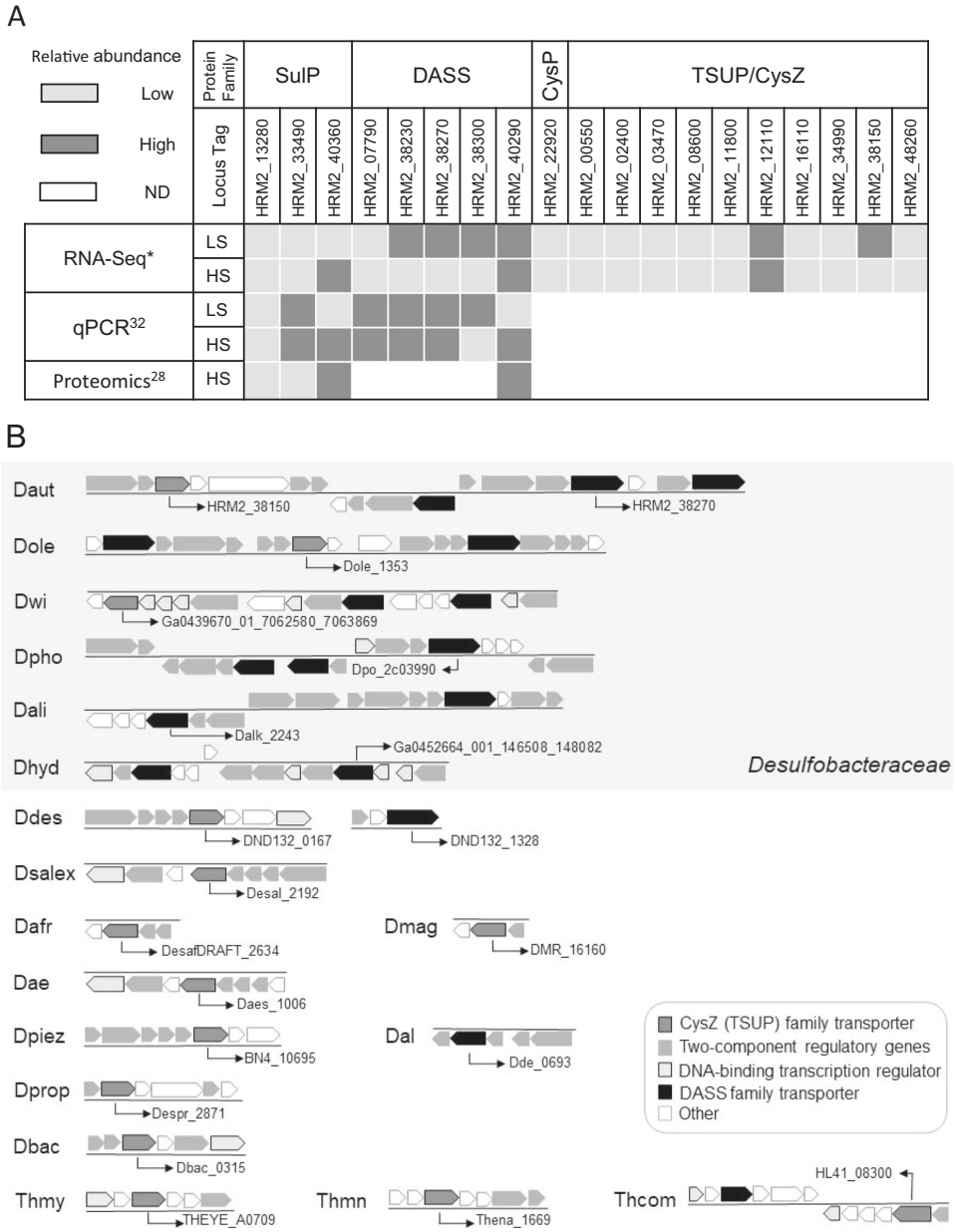

Fig. 4 Sulfate transporter genes in *D. autotrophicum*. A The relative abundance of putative sulfate transporters in *D. autotrophicum* in the presence of excess (HS) or limited (LS) concentrations of sulfate. ND not determined; * this study. **B** The genomic location of putative sulfate transporter genes and their proximity to two-component regulatory system genes. Daut HRM2 *D. autotrophicum,* Dwi *Desulfosarcina widdelii* PP31, Dpho *Desulfotignum phosphitoxidans* DSM13687, Dali *Desulfatibacillum aliphaticivorans* AK-01, Dhyd Desulfobacter hydrogenophilus, Ddes ND132, *Desulfovibrio desulfuricans* ND132, Dae *Pseudodesulfovibrio aespoeensis* Aspo-2, Dsalex *Desulfovibrio salexigens,* Dole *Desulfococcus oleovorans* Hxd3, Dprop *Desulfobulbus propionicus* 1pr3, Dbac *Desulfomicrobium baculatum* X, Dmag *Desulfovibrio magneticus* RS-1, Dal *Desulfovibrio alaskensis* G20, Dafr *Desulfovibrio africanus* Walvis Bay, Dpiez *Pseudodesulfovibrio piezophilus* C1TLV30, Thcom *Thermodesulfobacterium commune*, Thmn *Thermodesulfobium narugense* Na82, Thmy *Thermodesulfovibrio yellowstonii*.

results support earlier in silico predictions that TSUP transporters have a key role in the uptake of sulfate in SRM [33]. TSUP family transporter-encoding genes are abundant in SRM and they are the only putative sulfate transporters to be present in all SRM genomes examined, including bacterial and archaeal genomes [33]. Moreover, we recently described the presence of a TSUP family putative sulfate transporter on a plasmid of a marine SRM that exhibited high similarity to subseafloor-recovered metagenomic sequences, suggesting that TSUP high-affinity sulfate transporters might be important for survival under extreme sulfate limitation [78]. Previous "omics" approaches in SRM did not detect the overexpression of TSUP family gene transcripts or proteins. This further confirms that their expression is linked to sulfate limitation since the majority of previous studies were carried in excess of sulfate, detecting mainly the overexpression of SulP family transporters [28, 45, 63, 77]. Sulfate transporters are poorly characterized in SRM and our results on differential expression under highly controlled conditions offer a novel insight into the identity and regulation of sulfate transporters in SRM.

Most of the putative sulfate transporters were closely located, and in some cases co-transcribed, with TCR genes (Table S4). We examined the genomes of other SRM for the presence of TCR systems in close proximity to putative sulfate transporters and observed more examples, among a polyphyletic group of SRM from

freshwater and marine environments, where TCR can be found flanking TSUP and NadC/DASS family-encoding genes (Fig. 4B, Table S8). Several TCR systems have been identified in the model SRM, *Desulfovibrio vulgaris*, with putative roles, among others, in potassium and phosphate limitation response [79, 80].

The overexpressed TCR-encoding genes (Table S4) contain either a DNA-binding output domain, placing them in the nitrogen regulatory protein C (NtrC) family of response regulators, or CheY output domains, facilitating direct protein-protein interactions for chemotaxis [79]. Moreover, the putative NtrC family sensor kinases encoded by HRM2_38130, HRM2_38220, and HRM2_38250 share 32, 36, and 34% identity, respectively, with ZraS from *E. coli*, while the putative CheY family response regulators encoded by HRM2_38210 and HRM2_38240 shared 40 and 38% identity, respectively, with the *E. coli* ZraR (Table S4). ZraS and ZraR are part of a TCR system in *E. coli* that senses Zn^{2+} (ZraS) activating the regulation (ZraR) of genes involved in zinc homeostasis or protection against zinc toxicity [81]. Based on the proximity of these TCR systems and their conserved co-location across SRM genomes we therefore propose that, similarly in *D. autotrophicum*, TCR systems can sense changes in the sulfate concentration, regulate gene expression, and consequently affect the physiological response to sulfate limitation

CONCLUSION

D. autotrophicum responds to electron acceptor availability by switching between complete and incomplete lactate oxidation ("overflow" metabolism) and upregulating the expression of genes encoding transporters with high affinity for the limiting substrate. Both responses have been previoulsy described as key adaptations to low-energy life in marine sediments. Similarly, the C/N ratio controls the fate of nitrate in pure culture experiments and in situ [82, 83]. Low C/N ratios favor denitrification (electron donor limitation) as this process yields more energy per C oxidized compared to ammonification, while high C/N ratios (electron acceptor limitation) favor ammonification as this process yields more energy per nitrate reduced [82, 83]. Electron donor concentration also affects the metabolism of *Thiomicrospira sp.* CV0, that oxidizes sulfide with nitrate to sulfate at low in situ sulfide concentrations and to sulfur at high sulfide concentrations [84]. Diversity of carbon utilization and "overflow" metabolism may be critical for survival in low-energy environments such as marine sediments. SRM are able to oxidize the products of primary fermentation completely in the upper sulfate-rich marine sediments, while they likely switch to "overflow" metabolism (incomplete oxidation) releasing reducing equivalents to coexisting partners (i.e., methanogens) when sulfate becomes limited.

REFERENCES

1. Jørgensen BB. Mineralization of organic matter in the sea bed-the role of sulphate reduction. Nature. 1982;296:643–5.
2. Kasten S, Jørgensen BB. Sulfate reduction in marine sediments. In: Schulz H, Zabel M, editors. Marine geochemistry. Berlin: Springer; 2000. pp. 263–81.
3. Pellerin A, Antler G, Røy H, Findlay A, Beulig F, Scholze C, et al. The sulfur cycle below the sulfate-methane transition of marine sediments. Geochim Cosmochim Acta. 2018;239:74–89.
4. Reeburgh WS. Oceanic methane biogeochemistry. Chem Rev. 2007;107:486–513.
5. Holmkvist L, Ferdelman TG, Jørgensen BB. A cryptic sulfur cycle driven by iron in the methane zone of marine sediment (Aarhus Bay, Denmark). Geochim Cosmochim Acta. 2011;75:3581–99.
6. Starnawski P, Bataillon T, Ettema TJ, Jochum LM, Schreiber L, Chen X, et al. Microbial community assembly and evolution in subseafloor sediment. Proc Natl Acad Sci USA. 2017;114:2940–5.
7. Hoehler TM, Jørgensen BB. Microbial life under extreme energy limitation. Nat Rev Microbiol. 2013;11:83–94.
8. Jørgensen BB, Marshall IP. Slow microbial life in the seabed. Annu Rev Mar Sci. 2016;8:311–32.
9. Lever MA, Rogers KL, Lloyd KG, Overmann J, Schink B, Thauer RK, et al. Life under extreme energy limitation: a synthesis of laboratory-and field-based investigations. FEMS Microbiol Rev. 2015;39:688–728.
10. Button DK. Kinetics of nutrient-limited transport and microbial growth. Microbiol Rev. 1985;49:270–97.
11. De Mattos MT, Neijssel OM. Bioenergetic consequences of microbial adaptation to low-nutrient environments. J Biotechnol. 1997;59:117–26.
12. Egli T. How to live at very low substrate concentration. Water Res. 2010;44:4826–37.
13. Li J, Mara P, Schubotz F, Sylvan JB, Burgaud G, Klein F, et al. Recycling and metabolic flexibility dictate life in the lower oceanic crust. Nature. 2020;579:250–5.
14. Zinke LA, Mullis MM, Bird JT, Marshall IP, Jørgensen BB, Lloyd KG, et al. Thriving or surviving? Evaluating active microbial guilds in Baltic Sea sediment. Environ Microbiol Rep. 2017;9:528–36.
15. Orsi WD, Jørgensen BB, Biddle JF. Transcriptional analysis of sulfate reducing and chemolithoautotrophic sulfur oxidizing bacteria in the deep subseafloor. Environ Microbiol Rep. 2016;8:452–60.
16. Orsi WD, Edgcomb VP, Christman GD, Biddle JF. Gene expression in the deep biosphere. Nature. 2013;499:205–8.
17. Cappenberg TE. A study of mixed continuous cultures of sulfate-reducing and methane-producing bacteria. Microb Ecol. 1975;2:60–72.
18. Middleton AC, Lawrence AW. Kinetics of microbial sulfate reduction. J Water Pollut Control Fed. 1977;49:1659–70.
19. Nethe-Jaenchen R, Thauer RK. Growth yields and saturation constant of *Desulfovibrio vulgaris* in chemostat culture. Arch Microbiol. 1984;137:236–40.
20. Ingvorsen K, Zehnder AJ, Jørgensen BB. Kinetics of sulfate and acetate uptake by *Desulfobacter postgatei*. Appl Environ Microbiol. 1984;47:403–8.
21. Cypionka H, Pfennig N. Growth yields of *Desulfotomaculum orientis* with hydrogen in chemostat culture. Arch Microbiol. 1986;143:396–9.
22. Okabe S, Characklis WG. Effects of temperature and phosphorous concentration on microbial sulfate reduction by *Desulfovibrio desulfuricans*. Biotechnol Bioeng. 1992;39:1031–42.
23. Okabe S, Nielsen PH, Characklis WG. Factors affecting microbial sulfate reduction by *Desulfovibrio desulfuricans* in continuous culture: limiting nutrients and sulfide concentration. Biotechnol Bioeng. 1992;40:725–34.
24. Habicht KS, Salling L, Thamdrup B, Canfield DE. Effect of low sulfate concentrations on lactate oxidation and isotope fractionation during sulfate reduction by *Archaeoglobus fulgidus* strain Z. Appl Environ Microbiol. 2005;71:3770–7.
25. Davidson MM, Bisher ME, Pratt LM, Fong J, Southam G, Pfiffner SM, et al. Sulfur isotope enrichment during maintenance metabolism in the thermophilic sulfate-reducing bacterium *Desulfotomaculum putei*. Appl Environ Microbiol. 2009;75:5621–30.
26. Brysch K, Schneider C, Fuchs G, Widdel F. Lithoautotrophic growth of sulfate-reducing bacteria, and description of *Desulfobacterium autotrophicum* gen. nov., sp. nov. Arch Microbiol. 1987;148:264–74.
27. Strittmatter AW, Liesegang H, Rabus R, Decker I, Amann J, Andres S, et al. Genome sequence of *Desulfobacterium autotrophicum* HRM2, a marine sulfate reducer oxidizing organic carbon completely to carbon dioxide. Environ Microbiol. 2009;11:1038–55.
28. Dörries M, Wöhlbrand L, Rabus R. Differential proteomic analysis of the metabolic network of the marine sulfate-reducer *Desulfobacterium autotrophicum* HRM2. Proteomics. 2016;16:2878–93.
29. Petro C, Zäncker B, Starnawski P, Jochum LM, Ferdelman TG, Jørgensen BB, et al. Marine deep biosphere microbial communities assemble in near-surface sediments in Aarhus Bay. Front Microbiol. 2019;10:758.
30. Jochum LM, Chen X, Lever MA, Loy A, Jørgensen BB, Schramm A, et al. Depth distribution and assembly of sulfate-reducing microbial communities in marine sediments of Aarhus Bay. Appl Environ Microbiol. 2017;83:e01547–17.
31. Leloup J, Loy A, Knab NJ, Borowski C, Wagner M, Jørgensen BB. Diversity and abundance of sulfate-reducing microorganisms in the sulfate and methane zones of a marine sediment, Black Sea. Environ Microbiol. 2007;9:131–42.
32. Tarpgaard IH, Jørgensen BB, Kjeldsen KU, Røy H. The marine sulfate reducer *Desulfobacterium autotrophicum* HRM2 can switch between low and high apparent half-saturation constants for dissimilatory sulfate reduction. FEMS Microbiol Ecol. 2017;93:fix012.
33. Marietou A, Røy H, Jørgensen BB, Kjeldsen KU. Sulfate transporters in dissimilatory sulfate reducing microorganisms: a comparative genomics analysis. Front Microbiol. 2018;9:309.
34. Tarpgaard IH, Røy H, Jørgensen BB. Concurrent low-and high-affinity sulfate reduction kinetics in marine sediment. Geochim Cosmochim Acta. 2011;75:2997–3010.
35. Volpi M, Lomstein BA, Sichert A, Røy H, Jørgensen BB, Kjeldsen KU. Identity, abundance, and reactivation kinetics of thermophilic fermentative endospores in cold marine sediment and seawater. Front Microbiol. 2017;8:131.

36. Glombitza C, Pedersen J, Røy H, Jørgensen BB. Direct analysis of volatile fatty acids in marine sediment porewater by two-dimensional ion chromatography-mass spectrometry. Limnol Oceanogr Methods. 2014;12:455–68.
37. Glombitza C, Jaussi M, Røy H, Seidenkrantz MS, Lomstein BA, Jørgensen BB. Formate, acetate, and propionate as substrates for sulfate reduction in sub-arctic sediments of Southwest Greenland. Front Microbiol. 2015;6:846.
38. Reese BK, Finneran DW, Mills HJ, Zhu MX, Morse JW. Examination and refinement of the determination of aqueous hydrogen sulfide by the methylene blue method. Aquat Geochem. 2011;17:567.
39. Beulig F, Røy H, McGlynn SE, Jørgensen BB. Cryptic CH 4 cycling in the sulfate-methane transition of marine sediments apparently mediated by ANME-1 archaea. ISME J. 2019;13:250–62.
40. Thorup C, Schramm A, Findlay AJ, Finster KW, Schreiber L. Disguised as a sulfate reducer: growth of the deltaproteobacterium *Desulfurivibrio alkaliphilus* by sulfide oxidation with nitrate. MBio 2017;8:e00671–17.
41. Markowitz VM, Chen IM, Palaniappan K, Chu K, Szeto E, Grechkin Y, et al. IMG: the integrated microbial genomes database and comparative analysis system. Nucleic Acids Res. 2012;40:D115–22.
42. Rabus R, Venceslau SS, Wöhlbrand L, Voordouw G, Wall JD, Pereira IAC. Chapter two—a post-genomic view of the ecophysiology, catabolism and biotechnological relevance of sulphate-reducing prokaryotes. Adv Micro Physiol. 2015;66:55–321.
43. Finke N, Vandieken V, Jørgensen BB. Acetate, lactate, propionate, and isobutyrate as electron donors for iron and sulfate reduction in Arctic marine sediments, Svalbard. FEMS Microbiol Ecol. 2007;59:10–22.
44. Sonne-Hansen J, Westermann P, Ahring BK. Kinetics of sulfate and hydrogen uptake by the thermophilic sulfate-reducing bacteria *Thermodesulfobacterium* sp. strain JSP and *Thermodesulfovibrio* sp. strain R1Ha3. Appl Environ Microbiol. 1999;65:1304–7.
45. Keller KL, Wall JD. Genetics and molecular biology of the electron flow for sulfate respiration in *Desulfovibrio*. Front Microbiol. 2011;2:135.
46. Molenaar D, Van Berlo R, De Ridder D, Teusink B. Shifts in growth strategies reflect tradeoffs in cellular economics. Mol Syst Biol. 2009;5:323.
47. Vemuri GN, Altman E, Sangurdekar DP, Khodursky AB, Eiteman MA. Overflow metabolism in *Escherichia coli* during steady-state growth: transcriptional regulation and effect of the redox ratio. Appl Environ Microbiol. 2006;72:3653–61.
48. Meyer B, Kuehl JV, Price MN, Ray J, Deutschbauer AM, Arkin AP, et al. The energy-conserving electron transfer system used by *Desulfovibrio alaskensis* strain G 20 during pyruvate fermentation involves reduction of endogenously formed fumarate and cytoplasmic and membrane-bound complexes, Hdr-Flox and Rnf. Environ Microbiol. 2014;16:3463–86.
49. Noguera DR, Brusseau GA, Rittmann BE, Stahl DA. A unified model describing the role of hydrogen in the growth of *Desulfovibrio vulgaris* under different environmental conditions. Biotechn Bioengin. 1998;59:732–46.
50. Odom JM, Peck HD Jr. Hydrogen cycling as a general mechanism for energy coupling in the sulfate-reducing bacteria, *Desulfovibrio* sp. FEMS Microbiol Lett. 1981;12:47–50.
51. Lupton FS, Conrad R, Zeikus JG. Physiological function of hydrogen metabolism during growth of sulfidogenic bacteria on organic substrates. J Bacteriol. 1984; 159:843–9.
52. Jin Q, Bethke CM. Cellular energy conservation and the rate of microbial sulfate reduction. Geology. 2009;37:1027–30.
53. Hoskisson PA, Hobbs G. Continuous culture-making a comeback? Microbiology. 2005;151:3153–9.
54. Overbeek R, Fonstein M, D'Souza M, Pusch GD, Maltsev N. The use of gene clusters to infer functional coupling. Proc Natl Acad Sci. 1999;96:2896–901.
55. Hocking WP, Stokke R, Roalkvam I, Steen IH. Identification of key components in the energy metabolism of the hyperthermophilic sulfate-reducing archaeon *Archaeoglobus fulgidus* by transcriptome analyses. Front Microbiol. 2014;5:95.
56. Pereira IA, Ramos AR, Grein F, Marques MC, Da Silva SM, Venceslau SS. A comparative genomic analysis of energy metabolism in sulfate reducing bacteria and archaea. Front Microbiol. 2011;2:69.
57. Noji H, Yoshida M. The rotary machine in the cell, ATP synthase. J Biol Chem. 2001;276:1665–8.
58. Plugge CM, Scholten JC, Culley DE, Nie L, Brockman FJ, Zhang W. Global transcriptomics analysis of the *Desulfovibrio vulgaris* change from syntrophic growth with *Methanosarcina barkeri* to sulfidogenic metabolism. Microbiol. 2010; 156:2746–56.
59. Phadtare S. Recent developments in bacterial cold-shock response. Curr Issues Mol Biol. 2004;6:125–36.
60. Rabus R, Brüchert V, Amann J, Könneke M. Physiological response to temperature changes of the marine, sulfate-reducing bacterium *Desulfobacterium autotrophicum*. FEMS Microbiol Ecol. 2002;42:409–17.
61. Barker HA. Amino acid degradation by anaerobic bacteria. Annu Rev Biochem. 1981;50:23–40.
62. Zinser ER, Kolter R. Mutations enhancing amino acid catabolism confer a growth advantage in stationary phase. J Bacteriol. 1999;181:5800–7.
63. Wick LM, Quadroni M, Egli T. Short- and long-term changes in proteome composition and kinetic properties in a culture of *Escherichia coli* during transition from glucose-excess to glucose-limited growth conditions in continuous culture and vice versa. Environ Microbiol. 2001;3:588–99.
64. Vollmer AC, Bark SJ. Twenty-five years of investigating the universal stress protein: function, structure, and applications. In: Advances in applied microbiology. Academic Press; 2018. pp. 1–36.
65. Clark ME, He Q, He Z, Huang KH, Alm EJ, Wan XF, et al. Temporal transcriptomic analysis as *Desulfovibrio vulgaris* Hildenborough transitions into stationary phase during electron donor depletion. Appl Environ Microbiol. 2006;72:5578–88.
66. Schauder R, Preuß A, Jetten M, Fuchs G. Oxidative and reductive acetyl CoA/carbon monoxide dehydrogenase pathway in *Desulfobacterium autotrophicum*. Arch Microbiol. 1988;151:84–9.
67. Kumari S, Beatty CM, Browning DF, Busby SJ, Simel EJ, Hovel-Miner G, et al. Regulation of acetyl coenzyme A synthetase in. Escherichia coli J Bacteriol. 2000;182:4173–9.
68. Wang Q, Ou MS, Kim Y, Ingram LO, Shanmugam KT. Metabolic flux control at the pyruvate node in an anaerobic *Escherichia coli* strain with an active pyruvate dehydrogenase. Appl Environ Microbiol. 2010;76:2107–14.
69. Shimizu K, Matsuoka Y. Regulation of glycolytic flux and overflow metabolism depending on the source of energy generation for energy demand. Biotechnol Adv. 2019;37:284–305.
70. Verhagen MF, O'Rourke T, Adams MW. The hyperthermophilic bacterium, *Thermotoga maritima*, contains an unusually complex iron-hydrogenase: amino acid sequence analyses versus biochemical characterization. Biochim Biophys Acta. 1999;1412:212–29.
71. Rabus RA, Hansen TA, Widdel FR. Dissimilatory sulfate-and sulfur-reducing prokaryotes. Prokaryotes. 2006;2:659–768.
72. Santos AA, Venceslau SS, Grein F, Leavitt WD, Dahl C, Johnston DT, et al. A protein trisulfide couples dissimilatory sulfate reduction to energy conservation. Science. 2015;350:1541–5.
73. Buckel W, Thauer RK. Flavin-based electron bifurcation, ferredoxin, flavodoxin, and anaerobic respiration with protons (Ech) or NAD^+ (Rnf) as electron acceptors: a historical review. Front Microbiol. 2018;9:401.
74. Venceslau SS, Stockdreher Y, Dahl C, Pereira IAC. The "bacterial heterodisulfide" DsrC is a key protein in dissimilatory sulfur metabolism. BBA Bioenerg. 2014; 1837:1148–64.
75. Grein F, Ramos AR, Venceslau SS, Pereira IA. Unifying concepts in anaerobic respiration: insights from dissimilatory sulfur metabolism. BBA Bioenerg. 2013; 1827:145–60.
76. Stahlmann J, Warthmann R, Cypionka H. Na^+-dependent accumulation of sulfate and thiosulfate in marine sulfate-reducing bacteria. Arch Microbiol. 1991;155: 554–8.
77. Wöhlbrand L, Ruppersberg H, Feenders C, Blasius B, Braun HP, Rabus R. Analysis of membrane-protein complexes of the marine sulfate reducer *Desulfobacula toluolica* Tol2 by 1D blue native-PAGE complexome profiling and 2D blue native-/SDS-PAGE. Proteomics. 2016;16:973–88.
78. Marietou A, Lund MB, Marshall IP, Schreiber L, Jørgensen BB. Complete genome sequence of *Desulfobacter hydrogenophilus* AcRS1. Mar Genom. 2020;50:100691.
79. Zhang W, Culley DE, Wu G, Brockman FJ. Two-component signal transduction systems of *Desulfovibrio vulgaris*: structural and phylogenetic analysis and deduction of putative cognate pairs. J Mol Evol. 2006;62:473–87.
80. Rajeev L, Luning EG, Dehal PS, Price MN, Arkin AP, Mukhopadhyay A. Systematic mapping of two component response regulators to gene targets in a model sulfate reducing bacterium. Genome Biol. 2011;12:R99.
81. Taher R, de Rosny E. A structure-function study of ZraP and ZraS provides new insights into the two-component system Zra. Biochim Biophys Acta. 2020;1865: 129810.
82. Kraft B, Tegetmeyer HE, Sharma R, Klotz MG, Ferdelman TG, Hettich RL, et al. The environmental controls that govern the end product of bacterial nitrate respiration. Science. 2014;345:676–9.
83. Yoon S, Cruz-García C, Sanford R, Ritalahti KM, Löffler FE. Denitrification versus respiratory ammonification: environmental controls of two competing dissimilatory NO^{3-}/NO^{2-} reduction pathways in *Shewanella loihica* strain PV-4. ISME J. 2015;9:1093–104.
84. Greene EA, Hubert C, Nemati M, Jenneman GE, Voordouw G. Nitrite reductase activity of sulphate-reducing bacteria prevents their inhibition by nitrate-reducing, sulphide-oxidizing bacteria. Environ Microbiol. 2003;5:607–17.
85. Dalsgaard T, Bak F. Nitrate reduction in a sulfate-reducing bacterium, *Desulfovibrio desulfuricans*, isolated from rice paddy soil: sulfide inhibition, kinetics, and regulation. Appl Environ Microbiol. 1994;60:291–7.
86. Ingvorsen K, Jørgensen BB. Kinetics of sulfate uptake by freshwater and marine species of *Desulfovibrio*. Arch Microbiol. 1984;139:61–6.

ACKNOWLEDGEMENTS

The authors are grateful to J. Gijs Kuenen for his guidance in setting up and running anaerobic chemostats. The authors thank Volker Meyer, Lars B. Pedersen, Preben Sørensen, Anne Stentebjerg, Jeanette Pedersen, and Karina Bomholt Oest for technical support. Casper Thorup, Lars Schreiber, Jeff Cole, and Sofia S. Venceslau are kindly acknowledged for helpful discussions. CG was funded by a Marie-Curie Individual Fellowship (DEEP CARBON FLUX #327675). This work was supported by the Danish National Research Foundation [DNRF104], the European Research Council [ERC Advanced Grant #294200] and the Danish Council for Independent Research [DFF—7014-00196] to BBJ. Finally, the authors would like to thank our anonymous reviewers for their constructive comments that helped improve the paper.

AUTHOR CONTRIBUTIONS

AM, KUK, and BBJ designed the experiments. AM performed the experiments. CG performed the VFA measurements and thermodynamic calculations. AM, KUK, and CG analysed the data. AM prepared the paper. All co-authors commented on and provided substantial edits to the paper. BBJ obtained the funding for this work.

COMPETING INTERESTS

The authors declare no competing interests.

ADDITIONAL INFORMATION

Supplementary information The online version contains supplementary material available at https://doi.org/10.1038/s41396-021-01061-2.

Correspondence and requests for materials should be addressed to A.M.

Reprints and permission information is available at http://www.nature.com/reprints

Publisher's note Springer Nature remains neutral with regard to jurisdictional claims in published maps and institutional affiliations.